Clustering, Communication and Environmental Oscillations in Populations of Budding Yeast

Chris Stowers Brian Robertson Hyunju Ban Carl H. Johnson
Todd Young Erik M. Boczko *

July 25, 2008

Abstract

We describe how simple models of communication, consistent with known yeast physiological mechanisms, produce non-stationary, multimodal population densities, that are collected into an integer number of clusters. Theoretical analysis and numerical simulations demonstrate that the cell cycle progression of these clusters produces observable oscillation. We present experimental data that confirms the existence of clusters during autonomous oscillations.

1 Introduction

The periodic oscillation of physiologically relevant variables during yeast growth and division have been reported and studied for over 40 years [8, 12, 30, 31, 42, 44, 46, 49]. The physiologically observed variables have covered the full conceivable gamut of biological complexity and include dissolved oxygen, pH, carbon and nitrogen sources such as glucose, ethanol and ammonia, second messengers such as cAMP, the expression level of mRNA's, the activity of metabolic enzymes and indices of growth and division such as the percentage of cells budded and DNA content.

The observed oscillations are of broad interest in biology and chemical engineering for a number of reasons. The control of oscillation and the regulation of yeast metabolism has been an important theme in the chemical engineering literature devoted to the efficient management of bioprocess [4, 14, 18, 41]. The observation of oscillations are also of interest because they expose questions regarding the coordination of the cell cycle and metabolism, and the possible existence of clocks and pacemakers [23, 24, 25]. The existence of autonomous oscillations and their classification has been investigated and described with regard to intercellular communication [16, 34, 37].

Autonomous oscillations are far from universal however, and are only routinely reported in a few strains and within relatively narrow ranges of operating parameters. Apart from the

*Correspondence to erik.boczko@vanderbilt.edu, Ph: 615 936–6668, Fax: 615 936–1427

non-universality two central questions remain unanswered: What is the feedback mechanism that produces the oscillations, and how is it related to cell cycle progression.

The vast majority of growth conditions produce asynchronously dividing, exponentially growing cultures whose normalized population distribution is time invariant. Under the assumption of asynchronous, exponential growth, the population structure of a budding yeast culture is described by a continuous population density that declines exponentially with cell cycle position from G1 to M, and geometrically with age [26]. Very little is known about time periodic population structures. Most of the experimental studies that have described population structure have been related to the effort to understand the coordination of yeast volume growth and the sensing mechanisms that gates entry at start [31, 48]. The experimental studies of population structure have been limited by the arduous nature of the biophysical characterizations required for which there does not exist any standard, high accuracy methodology. An advantage of theory and computation is that it is straightforward to produce population density profiles as a function of arbitrary variables [40].

1.1 The Maintenance of Synchrony

Cell cycle synchrony in budding yeast is typically measured from a time series of the percentage of the cells in the population that are budded. Buds emerge at or near the G_1 to S transition and persist till division occurs. The bud site accumulates chitin that remains as a permanent scar that can be stained to provide a quantitative experimental measure of replicative age. The bud index can be affected in two ways. It can rise as cells become budded and it can decline as budded cells divide and/or as newly divided cells dilute the total population. In a dense and well mixed culture the dilution rate should have no effect on the bud index since removal through dilution is an unbiased linear process.

Strains of budding yeast exhibit an age dependent, volume growth variation, that strongly dephases cell cycle synchrony [40, 48] under most nutrient conditions and at most dilution rates. Daughter cells are smaller at division than their mothers and consequently have a longer G_1 traverse. Even a small but systematic difference in traverse will eventually lead a culture to desynchronize. Typically no more than three consecutive damping cycles of bud index synchrony can be achieved [6, 45] in the absence of the phenomenon of autonomous oscillation. The maintenance of synchrony in an actively growing culture therefore requires the existence of some mechanism to counteract the natural forces that tend to dephase cell cycle synchrony during growth and division [40]. Similar reasoning appears in slightly different language in [22].

Oscillatory behavior in yeast are typically grouped into two or three classes whose designations differ depending on the author [16, 37]. A description of the population structure within any of these classes remains an open and fundamental question. It is speculated that the very rapid NADH oscillations produced during anaerobic glycolysis *in-vivo* could not be observed in the absence of strict population synchrony. It has been demonstrated that acetaldehyde acts as a synchronizing agent in this oscillation [10].

It has been claimed that short period aerobic oscillations in the IFO 0233 strain occur without cell cycle oscillations. The literature supporting this claim is reviewed in [35, 37], and appears to originate with a single paper [38], that cites a negative result without data. In contrast, we

present data that short period aerobic oscillations identical to those reported are accompanied by measurable bud index oscillations, see Figure 11.

Several feedback mechanism have been proposed for the maintenance of cell cycle synchrony. Mechanisms involving metabolite feedback that operate on growth rate are particularly elegant [17]: Oscillating metabolite concentrations produce oscillating growth rates and these can act to locally stabilize synchronous trajectories like a focusing billiard. Based on solid experimental evidence [30, 49], it has been suggested [13, 30] that during long period aerobic oscillations a burst of glycolysis follows from the liberation of glucose from glycogen and trehalose at the G_1-S boundary. The ethanol produced by the population entering S-phase is proposed to accelerate the growth of cells in G_1. Whether or not this proposition is true, it is an example of what we will call an *Advance* model. In this model an agent secreted by a proportion of the population in one particular phase of the cell cycle advances the cell cycle progression of those cells earlier in the cycle. In the opposite case of a *Delay* mechanism, cells would slow or stop their cell cycle progression in response to a secreted factor or metabolite. Again, ethanol has been implicated as a source of delays. For instance, it has been demonstrated that above strain dependent critical concentrations, ethanol slows cell cycle progression [21], and references therein. In an extreme case of a delay mechanism, that might adequately be called *Blocking*, the progression of cells would stop. Such is the response of budding yeast to pheromones such as α-factor, that stop cell cycle progression at the G_1-S boundary. We observe that advances or delays can be produced by mechanisms involving communication, the end result of which are oscillations.

It is perhaps important to note that we are not focused here on the particular, intracellular details of how signals are integrated, on which genes are responsible, etc., but rather on the nature of the gross feedback mechanism that couples the cell cycle progression of individual cells and the physiological consequences at the population level that reinforce the mechanism to produce a stable oscillation. We report experimental results on oscillations in cultures of the strain IFO 0233 and Cen.PK 113. Our main contribution is to interpret these data in light of mathematical results that demonstrate that *Advance* or *Delay* models can organize the population density into non-stationary multimodal distributions to produce temporally coherent or pseudo-synchronized groups. The cell cycle progression of the clusters produce the observed environmental oscillations. The cell cycle progression of these clusters can be observed in realistic simulations and provide insight and testable hypothesis.

1.2 Clustering

We have observed that various forms of communication among cells, that result in either advances or delays, robustly leads to clustering of cells within the cell cycle. Clustering is defined as the temporal pseudo-synchronization of large sub-populations within the cell cycle. A cluster is a significant group of cells passing through cell-cycle milestones, such as budding or division, at nearly the same time. A cluster is akin to a group of runners, close together with respect to the total length of the track, and moving together with comparable speed.

That advances or delays can cause spontaneous polarization in subpopulations was already appreciated by muller et al. [30] in their work on the dynamics of population structure. Our contribution here is to highlight the generality of the notion, to systematize its analysis with

mathematical rigor, and to demonstrate the existence of clusters through the concordance of experiment and theory.

The robustness of the clustering mechanism is observed in at least the following three ways. First, clustering occurs across a wide variety of mathematical models as we shall describe, from extremely general to highly specific. Second it is generated by the very large class of advance or delay feedback mechanisms. Finally the appearance of clustering in response to these feedback mechanisms is insensitive to noise. These attributes are essential for observability.

We have considered several realizations of cell-cycle models, supposing only that the appearance of a thresholded population of cells in one cell cycle phase, S, effects the growth of cells in another, R. That is, if the integrated population density in the S phase is larger than the threshold T, then the cells in the R phase are either advanced or delayed depending on the operative feedback mechanism. We have labeled these two phases S in analogy with the hydrogen sulfide evolution models of short term oscillatory control [32, 47] and the responsive R phase. The specific number of clusters that form depends on the widths of the S and R phases and on the particular feedback mechanism. Of key importance is the necessity that if clustering occurs, then there are an integer number of clusters. This observation explains the periodic-looking behaviors seen in autonomous oscillations with periods that are integer divisors of the cell-cycle length.

In [42, 46, 49] and in the experimental data described below, the bud index oscillates with the same period as dissolved oxygen. Our data include a measurement of the total number of cells in the population as a function of time, that also oscillates with the same period. The anti-phase relationship between the bud index and the cell density unequivocally indicate the existence of clusters in accord with the mathematical results.

2 Models of Growth and Division

We have analyzed the dynamics of populations of budding yeast given various generic forms of feedback between the cells. In all of the cases that we have considered the feedback can be interpreted as resulting from communication among the cells. In fact, the structure of the feedback was chosen as a generalization of the physiologically observed mechanisms operative in real yeast cultures. In all of the cases that we have considered, feedback resulted in a non-stationary, multimodal population density that contained clusters. Clustering has also been hypothesized to result from feedback of a form different than what we have considered [50]. The genericity and naturality of these results provide for us strong evidence that *clustering exists in nature and is a robust phenomenon.*

2.1 Advance and Delay Models

The results of our analysis are summarized starting from the most general models that are devoid of all but the most basic features. It is well known that the cell cycles of many strains of budding yeast differ in range and duration according to replicative age [48]. In the most basic models we ignore these distinctions in order to simplify the analysis. These details are reintroduced in later models. Let S and R represent portions of the cell cycle as described

above. Typically we are assuming that the R phase precedes the S phase in the normal cell cycle progression. Let $\rho_S(t)$ and $\rho_R(t)$ represent the total population of cells in those respective phases of the cell cycle. Since the system is dynamic these quantities may vary with time t.

An *advance model* corresponds to the following rule: If the fraction of cells in S exceeds some threshold, i.e, $\rho_S(t) > T_r$, then all cells currently in R, $\rho_R(t)$, are instantaneously promoted to the beginning of S, where they resume normal growth.

A *delay model* corresponds to the rule: If the fraction of cells in S exceeds some threshold $\rho_S(t) > T_r$, then cells at the beginning of S are blocked from entry into the S-phase. The blocked cells resume normal growth when the condition $\rho_S(t) > T_r$, becomes false at some time t.

It may appear that these rules are too strict to be realistic. Below we consider graduated versions that display the same behavior. We note also that the mating pheromone α-factor behaves as a delay model as described.

Either of these rules will cause the population to become more dense in certain portions of the cell cycle and less dense in others. The introduction of this type of modal, wave like structure within an actively growing and dividing population represents a form of synchrony. We call a group of synchronized cells a *cluster*. If the number of cells in a cluster is large enough to exceed the threshold of the model, we call it a *critical cluster*. The number and the size of the population clusters within a yeast culture will translate directly into measurable properties. For instance the cell density profile will increase each time a cluster of cells passes through the M phase, and the bud index must increase each time a cluster passes into S-phase. Mathematically we have begun to characterize the number of clusters that a particular feedback will produce. Therefore the following theorems have practical and measurable significance.

In [3], the interested reader can find proofs of the following theorems that give an upper bound on the number of critical clusters that can form.

Theorem 2.1 *In an advance model no more than* $\lfloor (|R| + |S|)^{-1} \rfloor$ *critical clusters can persist.*

Theorem 2.2 *In a delay model no more than* $\lceil |S|^{-1} \rceil$ *critical clusters can persist.*

Here $\lfloor x \rfloor$ denotes the largest integer less than or equal to x and $\lceil x \rceil$ denotes the smallest integer larger or equal to x. Also, $|S|$ signifies the temporal length of the S phase.

It can be shown that not only the number of cluster is bounded above, but in certain circumstances it is also bound below. This means that clusters **must** form.

Theorem 2.3 *In a delay model, if the cells are initially homogeneously distributed about the cell cycle and the density exceeds twice the threshold,* T_r*, then exactly* $\lceil |S|^{-1} \rceil$ *clusters will develop and persist.*

2.2 Small Random Perturbations

The results described above would be far less interesting or relevant if they did not persist in the presence of noise. Random and independent changes in the cell cycle progression of

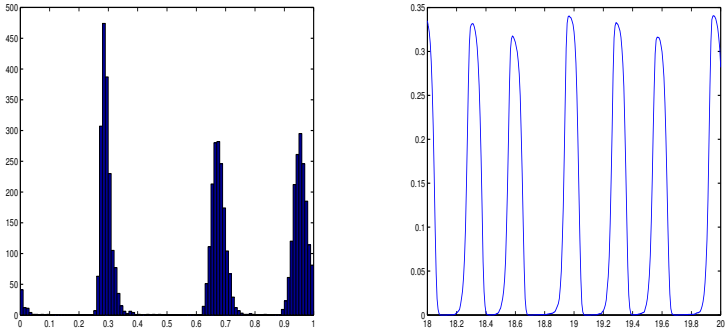

Figure 1: Simulations of the graduated model with acceleration. Here $R = [.1, .2]$, $S = [.2, .3]$, $\sigma = .02$ and the linear acceleration factor was 5. (LEFT) Histogram of the final distribution of cells within the cell cycles. (RIGHT) Time-series of the number of cells in the S-phase during the final two time frames. One unit of time corresponds to one unperturbed cell cycle.

individual cells will disperse any population synchrony in the absence of feedback. While there exist steady states with persistent clustering in noisy models the individual cells may migrate between clusters. Regardless, advance and delay models achieve clustering even in the presence of *small random perturbations* as the following theorem bears witness.

Theorem 2.4 *In a delay model with small stochastic perturbations, a homogeneous initial population whose total density exceeds* $2T_r/|S|$*, will form* $\lceil |S|^{-1} \rceil$ *critical clusters.*

2.3 Graduated but unstratified model.

In a graduated model we consider the possibility that the number of cells in S either act to slow down or accelerate cell growth of cells in an adjacent region R of the cycle.

Using a normalized, logarithmic scale, where 0 represents the beginning of the cell cycle and 1 its the end, we consider the following equations of motion:

$$\frac{dv}{dt} = \begin{cases} 1 + \xi & \text{if} \quad v \notin \mathrm{R} \\ 1 + F(\#\{\text{cells in S}\}) + \xi & \text{if} \quad v \in \mathrm{R}, \end{cases} \tag{2.1}$$

A cell that arrives at 1 immediately starts again at 0. This form is quite general since the functional dependence of F can take any functional form and the region R can be large or small. The term ξ models dispersion and we have considered Gaussian white noise, with variation σ. We have analyzed simulations of this model where F was assumed linear. For all parameter values considered we observed clustering, provided only that the noise is not too large. Figures 1 and 2 display the result that clustering occurred over the specified parameter values and in both graduated advance and delay models.

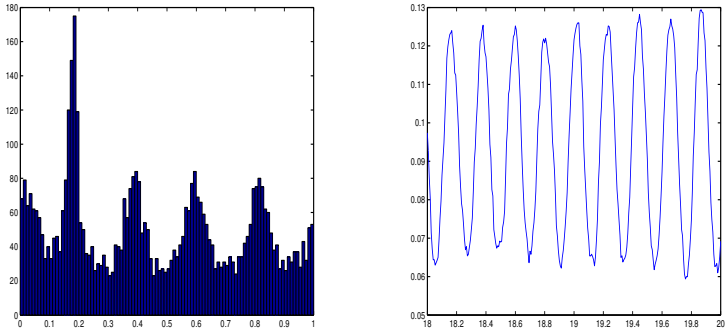

Figure 2: Simulations of the graduated model with inhibition. Parameters are the same as in Figure 1. (LEFT) Histogram of the final distribution of cells. (RIGHT) Time-series of the number of cells in the S-phase during the final two time frames.

2.4 Leslie Model Simulations

At the greatest level of detail we have considered models of budding yeast growth and division that are parameterized with experimental data and that are stratified with respect to cell cycle progression and age, see Figure 3. The data used to parameterize the model include age class dependent growth milestones such as the average size of a cell at bud emergence and the variance in that value. Such data are available in the literature for some strains [48], and we have made measurements for others. We have shown that these models can capture the complexity of yeast growth dynamics and account for strain variations therein [40].

In every model that we have examined, the simulation data clearly indicate that there exist open intervals of the threshold value in which synchronous cell cycle oscillations become stable in either advance or delay models. An examination of the population density shows that clustering occurs and that the cell cycle progression of the clusters with time is responsible for the oscillations.

Figure 4 shows the single cell oxygen profile used in the realistic flux model simulations shown in Figure 5. The flux model is outlined in Figure 3.

3 Material and Methods

Continuous Culture.

The haploid strain CENPK 113-7D(mat a) of budding yeast were cultivated in 3L New Brunswick Scientific Bioflow 110 reactor equipped with two Rushton type impellers, operated at 550 rpm. Air was sparged at a rate of 900 mL/min. Temperature was maintained at 30 degrees Celsius and pH was automatically controlled with 2 N sodium hydroxide.

Overnight cultures were grown in YPD media with shaking. 20mL were inoculated into a reactor containing 850 mL of synthetic media with the following composition: 10 gm per liter anhydrous glucose (Sigma G71528), 5 gm per liter ammonium sulfate (Sigma A2939), 0.5 gm

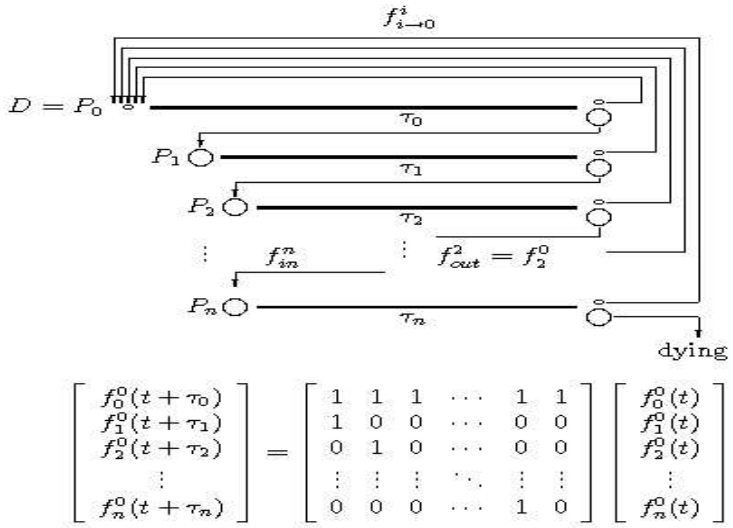

Figure 3: The division scheme and flux update equations used to propagate the budding yeast growth model. $f^i_{in}(t)$ is the total flux of cells entering the ith generation at time t. $f^0_i(t)$ are the total number of daughter cells produced from a division in age class i at time t. The values of the flux residence times, τ_k, are determined from experiment, see for instance Table 2, and describe the generational doubling times and length of individual cell cycles.

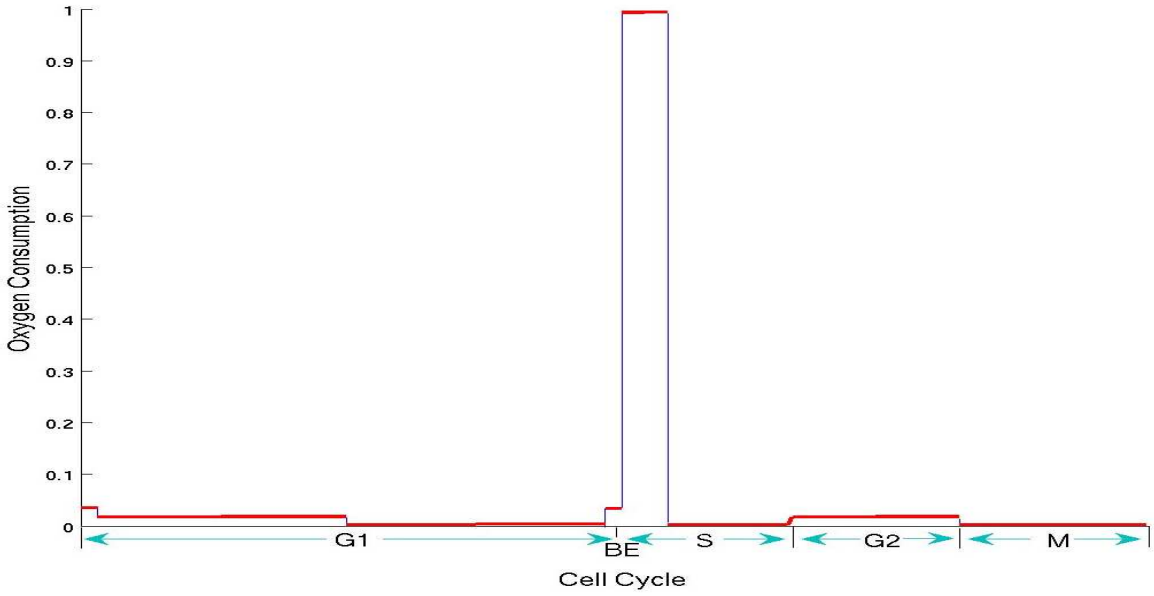

Figure 4: Single cell oxygen consumption profile used in the flux model simulations yeast growth and division. The figure shows how oxygen is consumed by the cell over the cell cycle. The result of using this profile are shown in Figure 7.

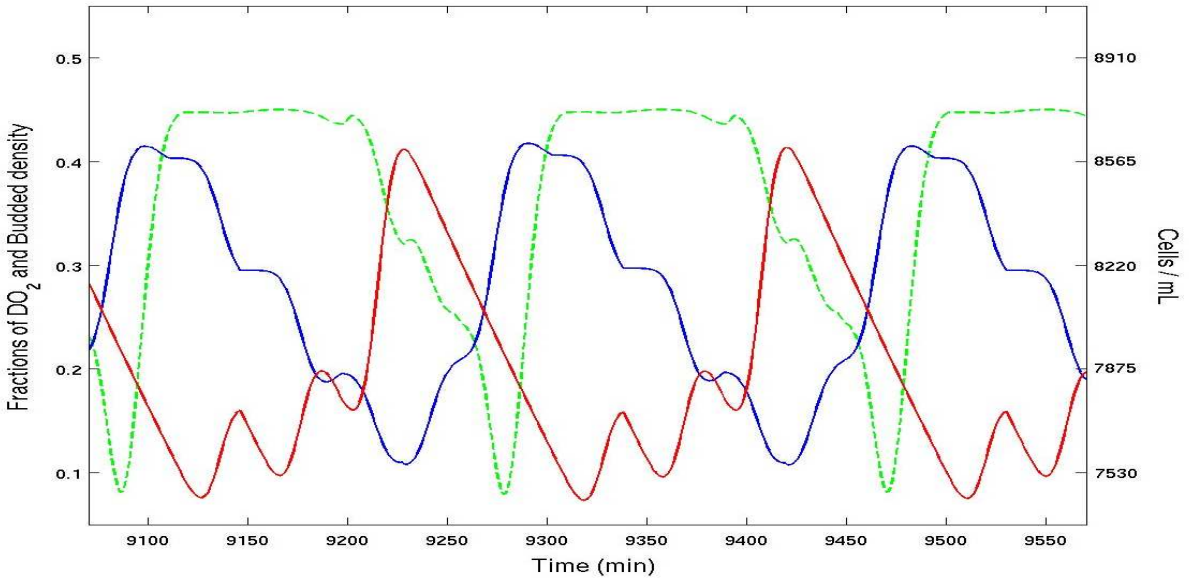

Figure 5: Dissolved O_2(green dashed), bud index(blue) and total cell number(red) oscillations as a function of time from a model simulation with a delay mechanism, see Figure 3. The simulation results recapitulate the observed experimental data seen in Figure 7.

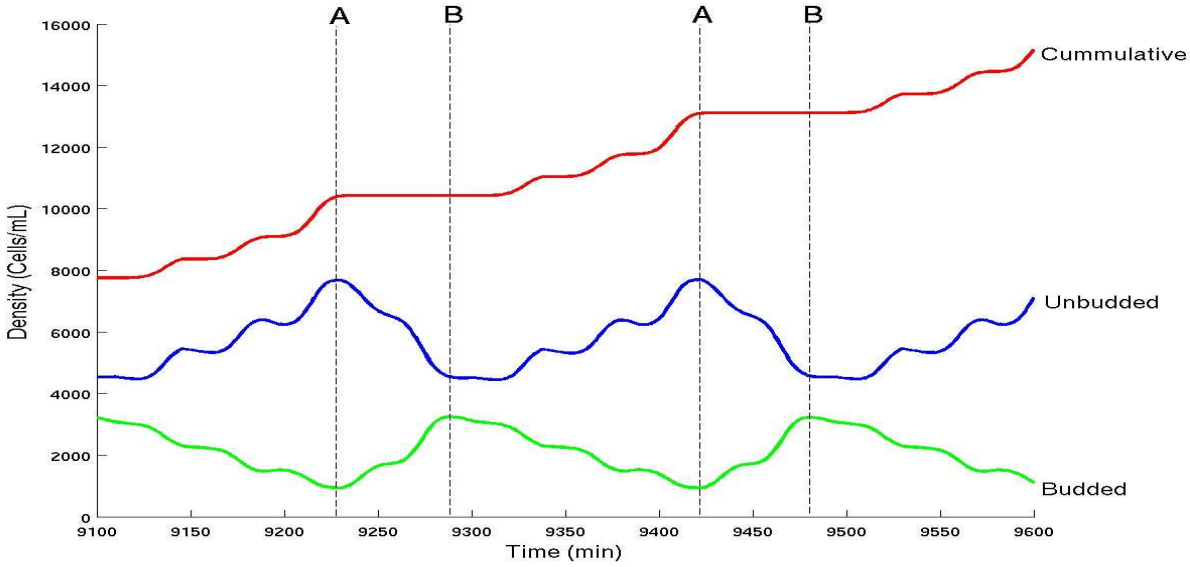

Figure 6: Cumulative cell density, budded and unbudded cell density as function of time for the simulation data shown in Figure 5. Two phases, a post-replicative phase A, and a pre-replicative phase B, are indicated by the dashed lines. It is observed that the A to B transition is shorter than the replicative transition B to A. The key difference between the simulation results and the corresponding experimental results shown in Figure 8 is that the simulation shows in greater detail small variations in density that arise from older generations.

per liter magnesium sulfate heptahydrate (Sigma M2773), 1 gm per liter of Yeast Extract (Becton, Dickinson and Company Cat 288620), 2 gm per liter potassium phosphate (Sigma P5379), 0.5 mL per mL of 70% v/v sulfuric acid, 0.5 mL of antifoam A (Sigma 10794), 0.5 mL of 250 mM calcium chloride, and 0.5 mL of mineral solution A, see Table 1.

Salt	Concentration
$FeSO_4 \bullet 7H_2O$	40gm/L
$ZnSO_4 \bullet 7H_2O$	20gm/L
$CuSO_4 \bullet 5H_2O$	10gm/L
$MnCl_2 \bullet 4H_2O$	2gm/L
75% H_2SO_4	20mL/L

Table 1: Mineral Solution A

The culture was subsequently grown in batch mode for 12-16 hours till it reached a cell density of approximately $5 \cdot 10^9$ cells/mL. Continuous culture ensued with a dilution rate of 0.088 per hour. Samples were taken from the reactor and flash frozen using dry ice.

The haploid strain IFO0223(mat a) require slightly different conditions. Overnight cultures were grown in YPD with shaking. 20 mL were inoculated into the reactor described above, containing 900 ml of the media previously described [23] with the exception that we used 0.5mL/L of Antifoam A. The reactor was perfused with wet air at rate of 200 mL/min, kept at pH of 3.4, and maintained an agitation speed of 750 rpm. The reactor was operated in batch mode for 16-20 hours. Operation was switched to continuous mode at a dilution rate of 0.087 per hour. Autonomous oscillations were obtained after switching to continuous mode following various hallmarks. These hallmarks include switching at the dissolved oxygen minimum, switching after it rebounded to 100% saturation, and following four hours of starvation. The cultures typically achieved a density of approximately $3 \cdot 10^8$ cells/mL.

Measurement of Bud Index and Cell Density

Cell samples were thawed in a 4°C sonicating water bath for 5 minutes and vortexed briefly. A μL of sample was resuspended in 10mL of Isoton Diluent(Sigma) and vortexed. The cell density of three independent half mL samples were measured using a Beckman Multisizer Coulter counter. The sizing threshold was 2-8μm.

Samples were stained with 1 mg/ml Primulin [36] for 5 minutes at room temperature, washed and resuspended in PBS. Bud scars were counted using a conventional Nikon TE-2000 microscope with a 100X objective and a DAPI fluorescence filter. No less than 100 cells were scored per frame. A minimum of three independent frames were scored per timepoint. The bud index was scored under white light from the same frame of cells used to count scars.

Generation	Fraction	τ_k
0	.5491	8.8
1	.2407	8.2
2	.1098	7.6
3	.0537	7.2
4+	.0467	—

Table 2: Age distribution data for CENPK growth during autonomous oscillation. The generational doubling times, τ_k, calculated from the age distribution are also shown.

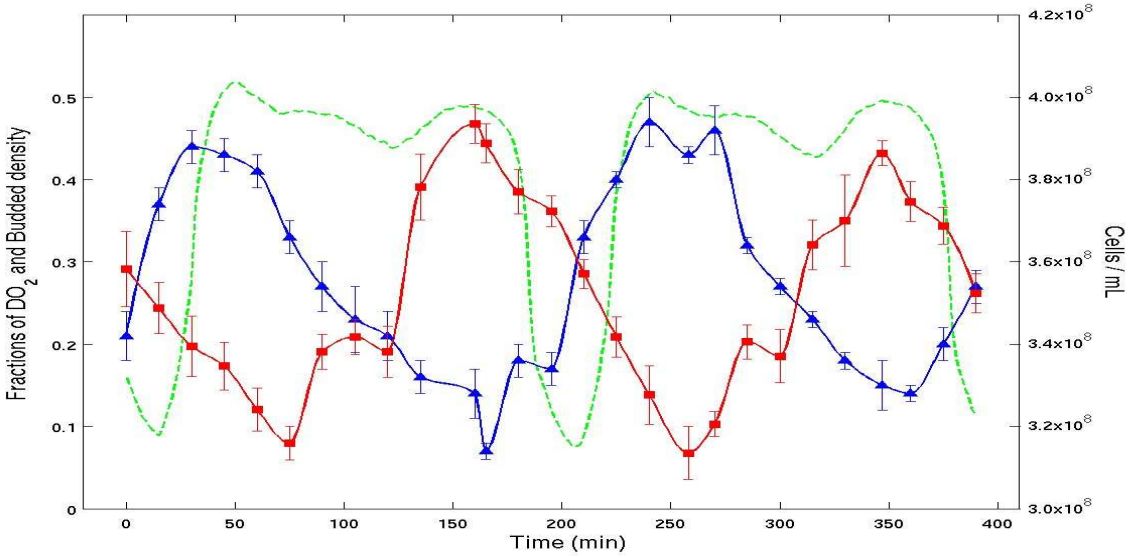

Figure 7: Dissolved O_2(green dashed), bud index(blue triangles) and total cell number(red squares) oscillations as a function of time during CENPK autonomous oscillation. Two oscillations occur within the approximate dilution rate doubling time of 6.86 hours. Error bars represent a standard deviation determined from triplicate repeats.

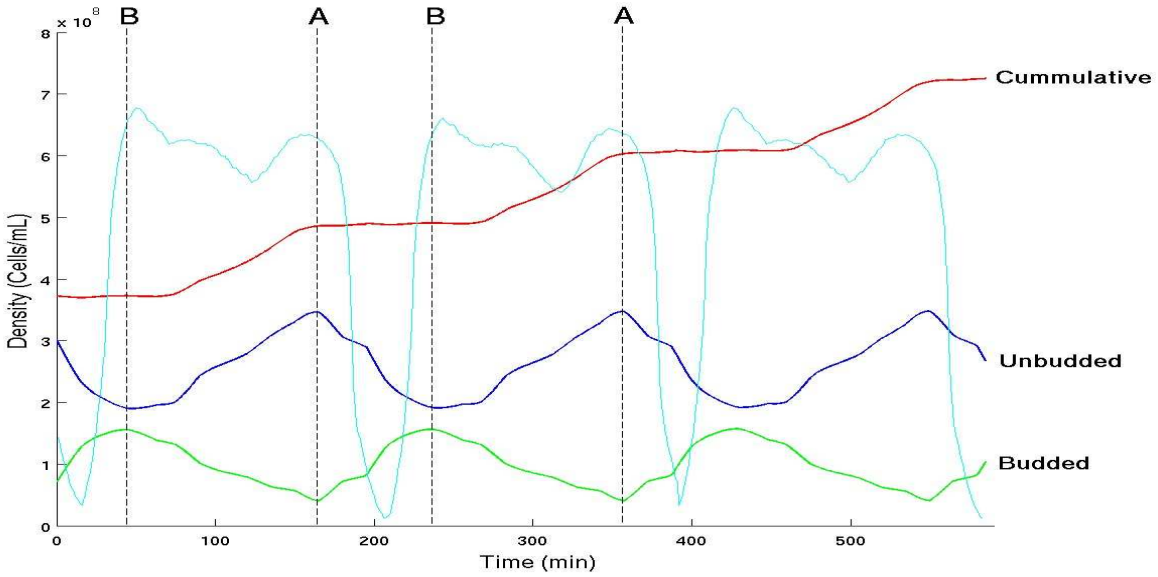

Figure 8: Cumulative cell density, budded and unbudded cell density as function of time for the experimental time series data shown in Figure 7. Two phases, a post-replicative phase A, and a pre-replicative phase B, are indicated by the dashed lines. It is observed that the A to B transition is shorter than the replicative transition B to A. The features of the density data clearly and naturally identify these periodic states and their transitions. The transitions between states correlate perfectly with those of the dissolved oxygen profile.

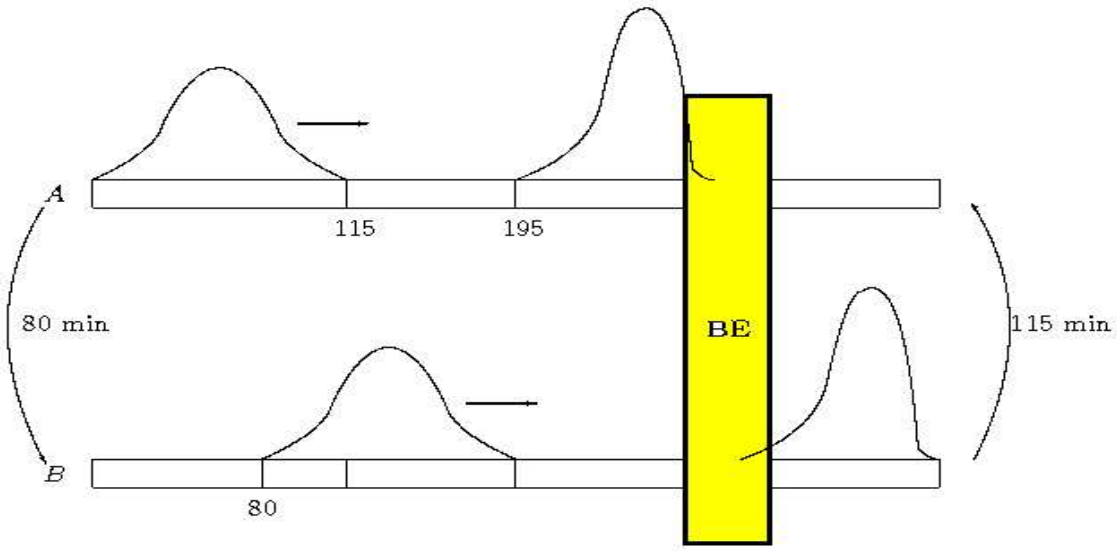

Figure 9: A model of the two phases of an oscillation that is consistent with all experimental and theoretical data. The timings reflect the details gleaned from the experimental time series data shown in Figures 7 and 8. The A state emerges after cell division with nearly all the cells in G_1. The rightmost cluster passes into the S-phase over the next 80 minutes as the A state passes into the B state. The G_1-S boundary lies within the yellow band labeled as bud emergence(BE). The rightmost cluster of cells divides as the B state returns to the A state, the previously leftmost cluster having reached the G_1-S-phase boundary. The course grained system exhibits period oscillation of the two states ABAB..., indefinitely.

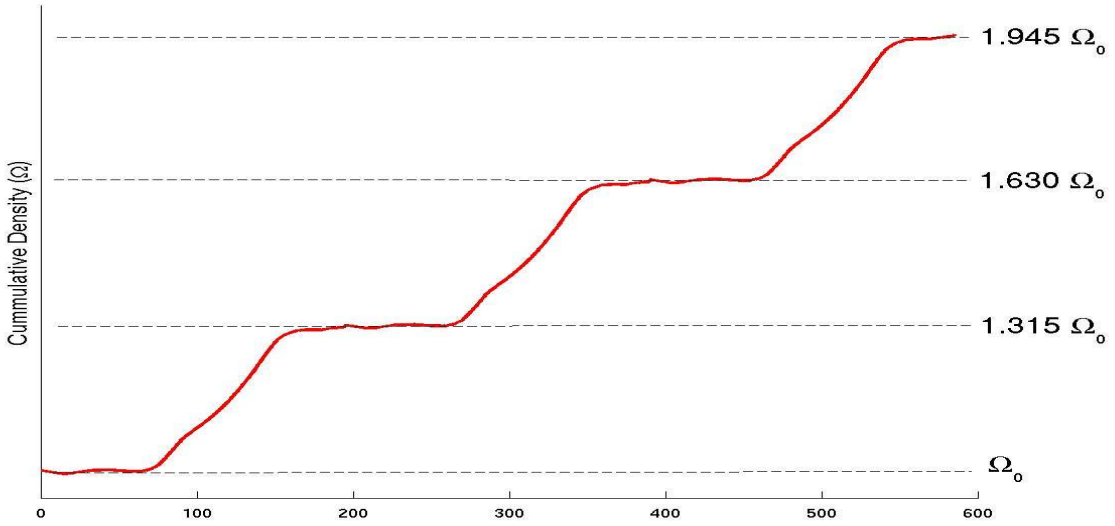

Figure 10: The cumulative density time series corresponding to the CENPK autonomous oscillation data shown in Figure 7 in red. The cumulative density increases in 31.5% fractions of the total. This is consistent with a synchronous system having two cell clusters as depicted Figure 9. The analysis behind this conclusion is described in the text.

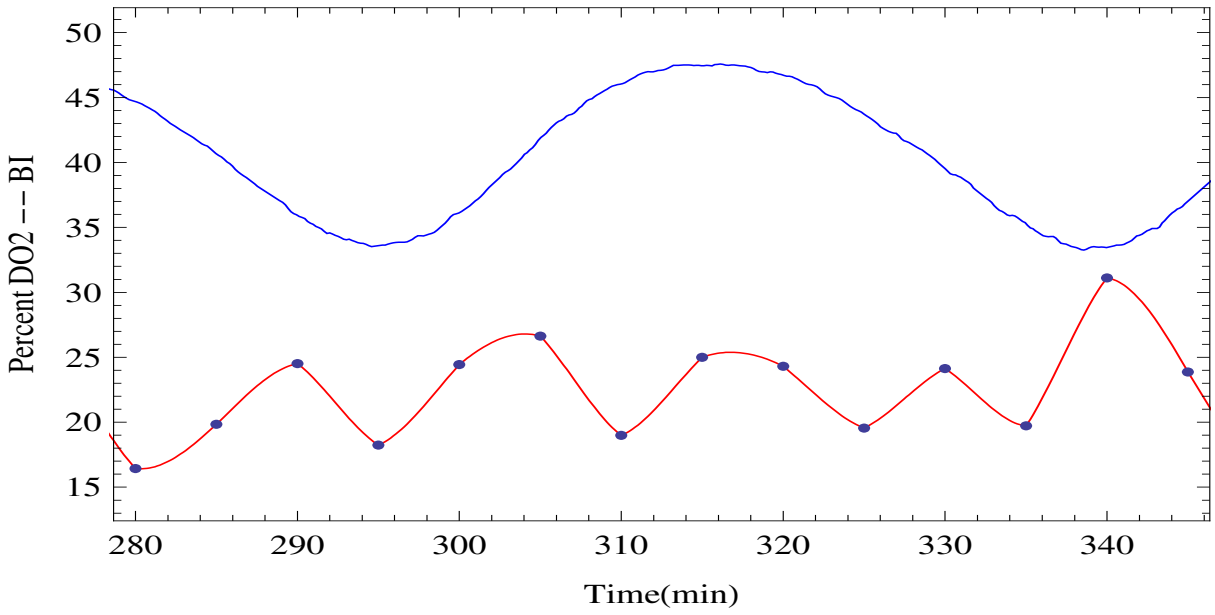

Figure 11: Bud index oscillation during short period aerobic oscillation in IFO 0223. The dissolved oxygen trace is shown in blue and exhibits a mean period of 39.4 ± 5.1 minutes. The bud index data are plotted as blue dots and interpolated with the red curve. The interpolated bud index exhibits a mean period of 14.2 ± 3.6 minutes.

4 Results

4.1 Existence of Clusters

Figure 7 shows three experimental time series collected over a 412 minute time period. The time series correspond to the dissolved oxygen trace, bud index oscillation and the cell density data. Two dissolved oxygen oscillations occur within the time period that corresponds to the doubling time of the dilution rate set in the experiment. Over the course of an oscillation the bud index percentage falls below 8%, and in a time span of 80 minutes rises to nearly 50%.

The fact that the bud index reaches nearly 50% and that this occurs twice within the culture doubling time shows that nearly half of the cells enter S-phase as a cluster, while the other half remain unbudded and reside in G_1. In the subsequent oscillation, the other half of the population density enters S-phase again as a cluster. The population density is organized into two clusters. Furthermore the data delimit two asymmetric phases within each oscillation, that naturally define both a symbol sequence and model of the population structure, see Figures 8 and 9.

The phase relationship of the density data to the bud index data is extremely informative. We draw the following conclusions. First, as the bud index rises to its maximum the cell density is purely in decline. From the slope of this decline we calculate a dilution rate that is within less that 8% error of the dilution rate set in the experiment, see also Figure 10. This is well within the deviation and statistical noise of the measurements and is strong evidence that no cell division is taking place as a cluster passes into the S-phase. The subsequent drop in bud index from its maximum value corresponds to a rise in cell density, indicating that loss of buds is due to cell division of that cluster.

Second, the phase relation between the cell density maximum and the subsequent bud index minimum, indicate that there exists a short period of time when both clusters coexists in the G_1 phase. Given the sampling rate, we can estimate this time to be on the order of 15 minutes. The magnitude of the bud index minimum, approximately 8%, is further indication of this temporal coexistence. The phase relation between these events represents the timing and spacing between the cell clusters, such that as the tail of the dividing cluster is passing through M-phase and all of its cells are returning to a G_1 phase, the second cluster's leading edge is passing into the S-phase and is beginning to bud.

Third, the close temporal interplay between the bud index minimum and the cell density maximum contains more information. The cells at the density max must be in early G_1. These same cells cannot begin to bud within the next fifteen minutes. The cells at the bud index minimum are doing just that. This indicates the existence of multiple clusters of cells. The fact that two oscillations occur within one dilution rate doubling time testifies to the interleaving of two clusters.

The temporal width of the bud index curve from its global maximum to the following global minimum indicates the width of the group of daughter cells that emerge within the P_0 generation due to the cell divisions. The temporal width is 115 minutes, Figure 7. The temporal distance from the bud index minimum to the following global maximum represents an upper bound on the time it takes the a cluster to pass into S-phase, and this time is 80 minutes. If the clusters are moving through the cell cycle at uniform speed then the differences in these

times reflect a narrowing of the daughter part of the cluster as it passes through G_1. There are several conceivable mechanisms that could effect this change. Since all cells do not bud at precisely the same cell cycle position or volume, the simultaneity induced by the dispersion in the budding process could account for some or all of the effect. We believe that this narrowing is at least in part an indication of the feedback mechanism that produces the clustered population structure by reducing the temporal variance within the the daughter population by 55-70% over the course of its G_1 traverse. While dilution will progressively whittle away at a cluster of cells throughout their cell cycle traverse, it cannot theoretically alter the width of the cluster at half-height. More data are required to further sharpen these deductions.

The symmetry of the bud index and cell density curves contain meaning. The fall in the bud index is not as sharp as its rise. Simulations indicate that the trailing tail is due to the fact that the different age classes do not divide in unison. This is supported by the fact that the cell density appears to have three distinct peaks, a fact also seen in simulations. This is also supported by generational doubling times calculated from the experimental age distribution data, see Table 2, that suggest that the length of the parent cell cycles become progressively shorter. Another observation is that the sharp rise in the bud index curve to its maximum could be indicative of a blocking mechanism near the G_1-S boundary. A blocking mechanism would cause cells to pile up along the leading edge of a cluster, while leaving a trailing tail, as observed.

4.1.1 Description of the Population Structure

From the data we can construct a description of the population structure and its dynamics. At the low point of the bud index one cluster of newly divided cells from the previous trailing tail are entering the early G_1 phase. Simultaneously the second cluster is leaving G_1 and entering the S-phase in the consecutive bud index upswing. The cluster entering S-phase is highly coherent relative to the length of the cell cycle. The sharp rise in the bud index indicates that the cluster has a fairly sharp leading edge. This state of the system is clearly identifiable from the data and in Figure 9 we have labeled this the A-state.

We consistently imagine cell cycle traverse from left to right. As the rightmost cluster buds the bud index rises and there is no accompanying rise in cell number. The budding transition lasts 80 minutes and ends in the B-state that is characterized by the bud index maximum. The following transition from the B-state back to the A-state is accompanied by cell division and is the longer of the two transitions.

As the bud index declines from its maximum value the long tail indicates a loss of coherence. This is either due to dispersion in the division times of individual cells or the staggered division of different age classes due to variations in the lengths of their cell cycles or a combination of both. The experimental age distribution data and an analysis of model simulations suggest that the tail results from the staggered division of different age classes due to variations in the lengths of their cell cycles. Over the following 115 minutes the rightmost cluster must undergo division since that is the only way to leave the budded state.

During this time period the other half of the cells began and ended in the unbudded state, that must be G_1, and therefore that cluster of cells must have been in G_1 during the whole period. The next rise in bud index level can only be ascribed to these cells since the cells in

the first cluster have clearly not had time to pass all the way through the G_1 phase and bud again. The second group of cells then enters S-phase as a strongly coherent cluster in the same way as the previous one. This leaves only a description of what happens to the cells during G_1. From the tiered decline in bud index level described above, a broad cell cluster enters G_1. Apparently as the cells pass through G_1, coherence is restored, resulting in a fairly tight cluster of cells that enter S-phase again.

4.2 Factors Consistent with Clustering

We present two lines of evidence that further support the hypothesis that the population structure is composed of two clusters of cells. First, from experimental age distribution data, and also from the combination of bud index and the cell density data, we have estimated the average lengths of the cell cycles of the different age classes. Second, by integrating the cell density data we can determine the relative increase in density per oscillation. A simplified analysis shows that the relative increase depends on the number of clusters in a predictable way. The data are consistent with two clusters.

The hypothesis of 2 cell clusters, as described in the previous section, is consistent only with cell-cycle lengths that are either nearly the same over the first few generations, or if the daughter cell cycle is approximately twice as long as that of the parents. If it were otherwise a cluster would become incoherent at cell division, because generations with significantly shorter cell cycles would "get ahead" of its cluster. With more than 2 clusters, this problem could be remedied by the cells in the faster generation falling roughly into another temporally advanced cluster. For instance if parent generations had cell cycle lengths which were roughly 2/3 of the cycle length for daughter, then 3 clusters could be supported. Or, if the ratio was 3/4 then 4 clusters could be supported.

Independent of the relationship between the lengths of the cell cycles of the individual age classes, the partitioning of the cell cycle phases, specifically the G_1-S-phase boundary, impacts the population dynamics. For the above description to be valid, it must be the case that cells spend more than half of their time in the G_1 phase. Otherwise, the two or more cluster picture, or any more dispersed profile, could not result in a bud index oscillation from nearly 0% to 50%. It has long been appreciated that metabolic alterations in cell cycle length prolong or contract G_1 [39]. Our modeling hypothesis of advances or delays are tacitly assumed to impact cells during their G_1 traverse. An analysis of the time-series data shown in Figure 7 indicates that there are two distinct phases to each oscillation. These phases can be distinguished from the data as a division phase, that we label by the transition $B \rightarrow A$, and a budding phase that we label by the transition $A \rightarrow B$. The state A corresponds to the bud index minimum just prior to the dissolved oxygen minimum and the state B corresponds to the bud index maximum. The dynamic iteration of these states is envisioned in Figure 9, a pair of transitions mark each oscillation and four transitions fill a single dilution doubling time. The $A \rightarrow B$ transition is the shorter of the two.

The data suggest a model in which the cells spend roughly 65% of the time in G_1. The time average bud index, F, calculated from the experimental data is roughly 27-28%. Given that the population density is periodic it can be shown that the time average density remains proportional to $\exp(-Dt)$, where D is the dilution rate, $DP = \ln(2)$, and t represents cell cycle

position. Given this representation of the average population density, the estimated average time of bud emergence relative to the average cycle time is given by the formula: $\frac{t_b}{P} = \frac{\ln(\frac{2}{1+F})}{\ln(2)}$. These data and calculations indicate that, on average, bud emergence takes place 267 minutes into the 412 minute cycle shown in Figure 7.

In [2] an algorithm is derived to find the lengths of the cell cycles of the various generations from age distribution data. In Table 2 the first column is the replicative age and the second is the fraction found of that generation in the population. The third column is the length of cell cycles for each generation calculated from the age distribution using the algorithm of [2]. The known dilution rate doubling time is assumed in the calculation. If the τ_k values were equal across all generations, k, then the age distribution at steady state would be exactly geometric with $r = 0.50$, i.e. each generation should be half as numerous as the generation preceding it. For the measured age distribution we find almost exactly a geometric progression, but with $r = 0.46$. The values of τ calculated from the data indicate that the discrepancy of timespan between the daughter and first parent generations is about 0.6 hours or a percentage difference of 7%. These two generations together account for 79% of the total density. Simulations based on the derived cycle times and a blocking mechanism are able to reproduce the experimental data, see Figure 5.

Any system with a periodic, multimodal, population density cannot double within a dilution rate doubling time. This is because in such a system the total population density must oscillate and during some periods of time little or no population divisions occur. During these times, dilution prevails. Let $T_n(x)$ represent the total population density of an idealized system with n synchronous clusters. Then the function $F_n(z) := T_n(z) + D\int_0^z T_n(x)dx$ represents the accumulated density adjusted for effluent loss due to dilution. If $T(x) = Ke^{-Dx}$ then F will double exactly in one period P. In contrast, calculations of the behavior of the function F_n based on idealized synchronous systems indicate that systems with n humps will jump in density in fractions of the total that depend on n: $(1 - e^{-D/n})$. For two clusters the system jumps 29% of the total with each hump, and requires three oscillations to double. A system with three clusters is expected to jump only 20% per hump, and require roughly five oscillations to double. An analysis of our experimental data, indicates that the total density increases 31.5% per oscillation, see Figure 10. This is fully consistent with two clusters of cells.

5 Conclusions

Mathematical modeling, analysis and simulation show that advance and delay feedback mechanisms can initiate clustering over a wide range of parameter values and initial conditions. The conclusion is that clustering is a robust phenomenon that could arise from quorum sensing.

The Bud index data along with the cell density data in the Cen.PK strain show conclusively that clustering occurs. The experimental evidence presented in Figure 7 supports the conclusion that two independent critical clusters exist each containing roughly half the total cells. Further, the clustering of the population density and its subsequent cell cycle progression accounts for the observed O_2 oscillations.

The Leslie model simulations of a delay model shown in Figures 5 and 6, agree both qualita-

tively and quantitatively with the corresponding experimental data shown in Figures 7 and 8. The simulations provide a prediction of the dynamic progression of the clusters and a detailed picture that is instructive to interpret experimental results and to design experiments that progressively reveal the finer structure and coordination between metabolism, communication and clustering.

What remains unresolved are the specific details of the feedback mechanism that entrains the cells. While oxygen has been shown to act as a quorum sensing molecule [], and interesting hypothesis have been advanced for why it might act in that capacity in the Cen.PK oscillations [8, 42], its involvement in the hierarchy of cause and effect has not been convincingly elucidated. It is likely that multiple agents are involved.

Our hypothesis, consistent with the data is that the cell cluster that is approaching the G_1-S boundary, in the A-state, is secreting a synchronizing agent that acts on the newly emerged cluster in early G_1. Its is not clear if the feedback is only sensed by daughter cells or by by cells in G_1 of all ages. It is possible that cohesion established among daughter cells is maintained well enough with age that the system as a whole remains cohesive, coupled with the fact that successive generations decay in population density geometrically. The fact that the population structure is robustly altered by pH in a way that is qualitatively different from dilution indicates that communication is involved [4].

While our aim is to understand the population structure, we remark in conclusion on the connection between the population dynamics and the metabolic dynamics encoded in the dissolved oxygen oscillation. The data shown in Figure 8 clearly indicate that the utilization of dissolved oxygen occurs during the A to B transition. The B to A transition is marked by cell division. The data are consistent with G_1 phase oxidative metabolism and the supposed bonfire of storage carbohydrates that precedes start in slowly growing aerobic cultures [13, 30, 31, 49]. Since G_1 is the only phase without buds, the bud index minima and cell density maximum indicate that from 85-95% of the cells are in G_1 prior to the large downswing in dissolved oxygen. The minimum in the bud index occurs as a cohort of newly divided cells appear as a uniform cluster in the G_1 phase. At the same time the leading edge of the second cluster reaches bud emergence. At the dissolved oxygen minimum, slightly more than half the cluster has budded and the cell density profile shows only loss due to dilution, indicating that all cell division has ceased.

The connection between cell cycle synchrony and metabolic synchrony is a topic of great interest. Based on the evidence and our point of view, we hypothesize that the causal and logical connections are these. Actively dividing cells must be progressing through their cell cycle. Secreted by-products of metabolism accumulate in the culture media and at high enough cell density the metabolic response of the cells to their presence induces advances and/or delays in their cell cycle progression, that depend on the cell cycle position of the receiving cell. The existence of this feedback mechanism can causes a periodic population structure to emerge that is characterized by clusters of cells that progress through the cell cycle together provided that the lengths of the cell cycles of the generations are compatible. The periodic cell cycle progression of the clusters results in an overall population synchrony can be observed as oscillations in environmental variables.

The only evidence that autonomous oscillation and cell cycle progression are not intimately connected are dubious. We have raised the potentially contentious point that the so called

short period aerobic oscillations in the UFO 0223 strain, that have been reported to appear in the absence of cell cycle oscillations when the cells are grown in limiting glucose or ethanol, is unsubstantiated by the (UN)published data. We have provided bud index data, Figure 11, that clearly show that oscillations occur within the window of dilution rates for which it has been claimed otherwise without data.

Acknowledgment The authors dedicate this work to the memory of Robert Klevecz. EMB,CCS,HB were partially supported through NSF-DMS 0443855, NSF-ECS 0601528 and the short lived W.M. Keck Foundation Grant#062014. CHJ and BR acknowledge support from NIGMS GM-067152.

References

[1] H. Ban, E. Boczko, C. Stowers, Simulations of Yeast Culture Oscillations with a Full Leslie Model. Preprint 2008.

[2] H. Ban, E. Boczko, Age distribution formulas for budding yeast. Preprint 2008.

[3] E. Boczko, T. Gedeon, B. Klevecz, C. Stowers and T. Young, Advance and delay models and cell cycle clustering in yeast. Preprint 2008.

[4] M.Buese, A.Kopmann, H.Diekmann, M.Thoma, Oxygen, pH value, and carbon source induced changes of the mode of oscillation in synchronous continuous culture of *Saccharomyces cervisiae*. (1998). *Biotechno. Bioeng.* **63**:410-417.

[5] E.Boye, T.Stokke, N.Kleckner, and K.Skarstad, Coordinating DNA replication initiation with cell growth: Differential roles for DnaA and SeqA proteins. (1996) *Proc. Natl. Acad. Sci.* **93**:12206-12211.

[6] L.L.Breeden, α-Factor synchronization of budding yeast. (1997) *Methods in Enzymology* **283**:332-342.

[7] H.Chen, M.Fujita, Q.Feng, J.Clardy, and G.R.Fink, Tyrosol is a quorum sensing molecule in *Candida albicans*. (2004) *Proc. Natl. Acad. Sci.* **101**:5048-5052.

[8] Z.Chen, E.A.Odstrcil,B.P.Tu, S.L.McKnight, Restriction of DNA replication to the reductive phase of the metabolic cycle protects genome integrity. (2007) *Science* **316**:1916-1919.

[9] J.Collier, H.H.McAdams, and L.Shapiro, A DNA methylation ratchet governs cell cycle progression through a bacterial cell cycle. (2007) *Proc. Natl. Acad. Sci.* **104**:17111-17116.

[10] S.Dano, P.G.Sorensen and F.Hynne, Sustained oscillations in living cells. (1999) *Nature* **402**:320-322.

[11] G.M.Dunny, B.A.B.Leonard, Cell cell communication in Gram Positive bacteria. (1997) *Annu. Rev. Microbiol.* **51**:527-564.

[12] R.K.Finn, and R.E.Wilson, (1954) *Agric. Food Chem.* **2**:66-

[13] B.futcher, Metabolic cycle, cell cycle and the finishing kick to start. (2006) *Genome Biology* **7**:107-111.

[14] E.Heinzle, I.J.Dunn, K.Furakawa, and R.D.Tanner, Modeling of sustained oscillations observed in continuous culture of *Saccharomyces Cerevisiae*. (1982) in *Modeling and control of biotechnical processes* 1st IFAC Workshop:57-65.

[15] B.A.Hense, C.Kuttler, J.Muller, M.Rothballer, A.Hartmann, and J.Kreft, Does efficiency sensing unify diffusion and quorum sensing? (2007) *Nat. Rev. Microbiol.* **5**:230-239.

[16] M.A.Henson, Cell ensemble modeling of metabolic oscillations in continuous yeast cultures. (2005) *Comput. Chem. Enginer.* **29**:645-661.

[17] M.A.Hjortsø, and J.Nielsen, A conceptual model of autonomous oscillations in microbial cultures (1994). *Chemical Engineering Science*, **49**:1083-1095.

[18] M.A.Hjortsø, Population balance models of autonomous periodic dynamics in microbial cultures. Their use in process optimization. (1996). *Can. J. Chem. Engin.*, **74**:612-620.

[19] J.M.Hornby, E.C.Jensen, A.D.Lisec,..., and K.W.Nickeron, Quorum sensing in the dimorphic fungus *Candida albacans* is mediated by farnesol. (2001) *Appl. Environ. Microbiol.* **67**:2982-2992.

[20] K.D.Jones and D.S.Kompala, Cybernetic model of the growth dynamics of *Saccharomyces cervisiae* in batch and continuous culture. (1999) *J. Biotechnol.* **71**:105-131.

[21] R.P.Jones, Biological principles for the effects of ethanol. (1989) *Enzyme Microb. Technol.* **11**:130-153.

[22] M.Keulers, A.D.Satroutdinov, T.Sazuki, and H.Kuriyama, Synchronization affector of autonomous short period sustained oscillation of (1996) *Saccharomyces cerevisiae. Yeast* **12**:673-682.

[23] R. R. Klevecz, Quantized generation time in mammalian cells as an expression of the cellular clock. (1976) *Proc. Natl. Acad. Sci.* **73**:4012-4016.

[24] R. R. Klevecz, S.A.Kaufman, and R.M.Shymko, Cellular clocks and oscillators. (1984) *Inter. Rev. Cytol.* **86**:97-128.

[25] R. Klevecz, and D. Murray, Genome wide oscillations in expression, (2001) *Molecular Biology Reports* **28**:73-82.

[26] Lord, P.G., and Wheals, A.E. Asymmetrical division of *Saccharomyces cerevisiae.* (1980) *J. Bacter.* **142**:808-818.

[27] G.J.Lyon, R.P.Novick, Peptide signaling in *Staphylococcus aureus* and other Gram positive bacteria. (2004) *Peptides* **25**:1389-1403.

[28] E.E.N.Macau, and C.Grebogi, Driving trajectories in complex system. (1999) *Phys. Rev. E.* **59**:4062-4070.

[29] M.R.Mashego, M.L.A. Jansen, J.L.Vinke, W.M.van Gulik, J.J.Heijnen, Changes in the metabalome of *Saccharomyces cervisiae* associated with evolution in aerobic glucose-limited chemostats. (2005) *FEMS Yeast Res.* **5**:419-430.

[30] D.Muller, S.Exler, L.Aguilera-Vazquez, E.Guerrero-Martin, and M.Reuss, Cyclic AMP mediates the cell cycle dynamics of energy metabolism in *Saccharomyces cervisiae.* (2003) *Yeast* **20**:351-367.

[31] T.Munch, B.Sonnleitner, and A.Fiechter, The decisive role of the *Saccharomyces cervisiae* cell cycle behavior for dynamic growth characterization. (1992) *J. Biotechnol.* **22**:329-352.

[32] D. Murray, R. Klevecz, and D. Lloyd, Generation and maintenance of synchrony in *Saccharomyces cerevisiae* continuous culture, (2003), *Experimental Cell Research* **287**:10-15.

[33] Z.Palkova, J.Forstova, Yeast colonies synchronize their growth and development. (2000) *J. Cell Science* **113**:1923-1928.

[34] Z.Palkova, L.Vachova, Life within a community: benefits to yeast long term survival. (2006) *FEMS. Microbiol. Rev.* **30**:806-824.

[35] P.R.Patnaik, Oscillatory metabolism of *Saccharomyces cerevisiae*: An overview of mechanisms and models. (2003) *Biotechnology Advances* **21**:183-192.

[36] J.R.Pringle, Staining of bud scars and other cell wall chitin with calcoflour. (1991) *Methods In Enzymology* **194**:732-735.

[37] P.Richard, The rythm of yeast. (2003) *FEMS Microbiol. Rev.* **27**:547-557.

[38] A.D.Satroutdinov, H.Kuriyama, and H.Kobayashi, Oscillatory metabolism of *Saccharomyces cerevisiae* in continuous culture. (1992) *FEMS Microbiology Lett.* **98**:261-268.

[39] R.A.Singer, and G.C.Johnston, Nature of the G_1 phase of the yeast *Saccharomyces cerevisiae*. *Proc. Natl. Acad. Sci* **78**:3030-3033.

[40] C.Stowers, D.Hackworth, T.Gedeon, K.Mischaikow, and E. M. Boczko. Extending cell cycle synchrony and deconvolving population effects in budding yeast through an analysis of volume growth with a structured Leslie model. (2008) *Theor. Pop. Biol.* In Revision.

[41] C.Stowers, J. B. Robertson, H. Ban, R. D. Tanner, and E. M. Boczko (2008) Periodic Fermentor Yield and Enhanced Product Enrichment from Autonomous Oscillations. *Applied Biochemistry and Biotechnology.* To Appear.

[42] B.P.Tu, A.Kudlicki, M.Rowicka, S.L.McKnight, Logic of the yeast metabolic cycle: temporal compartmentation of cellular processes. (2005) *Science* **310**:1152-1158.

[43] T.Tvegard, H.Soltani, H.C.Skjolberg, M.Krohn, E.A.Nilssen, S.E.Kearsey, B.Grallert, and E. Boye, A novel checkpoint mechanism regulating the G1/S transition. (2007) *Genes and Development* **21**:649-654.

[44] K.Von Meyenburg, Stable synchronous oscillations in continuous cultures of S. cerevisiae under glucose limitation. (1973) in B.Chance (Ed) *Biological Biochemical Oscilllators* Academic Press, NY. 411.

[45] Walker G. Synchronization of yeast cell populations. (1999) *Methods in Cell Science* **21**:87-93.

[46] J.Wang, W.Liu, T.Uno,H.Tonozuka, K.Mitsui, K.Tsurugi, Cellular stress response oscillate in synchronization with the ultridian oscillation of energy metabolism in the yeast *Saccharomyces cervisiae*. (2000) *FEMS Microbiol. Lett.* **189**:9-13.

[47] J.Wolf, H-Y.Sohn, R.Heinrich, H.Kuriyama, Mathematical analysis of a mechanism for autonomous oscillations in a continuous culture of *Saccharomyces cerevisiae*. (2001) *FEBS Lett.* **499**:230-234.

[48] Woldringh CL, Huls PG, and Vischer NOE. Volume growth of daughter and parent cells during the cell cycle of *Saccharomyces cerevisiae* a/α as determined by image cytometry. (2003) *J. Bacteriology* **175**:3174-3181.

[49] Z.Xu, K.Tsurugi, A potential mechanism of energy metabolism oscillation in an aerobic chemostat culture of the yeast *Saccharomyces cervisiae*. (2006) *FEBS Journal* **273**:1696-1709.

[50] G.Zhu, A.Zamamiri, M.A.Henson, M.A.Hjortsø, Model predictive control of continuous yeast bioreactors using cell population balance models. (2000) *Chemical Engineering Science* **55**:6155-6167.